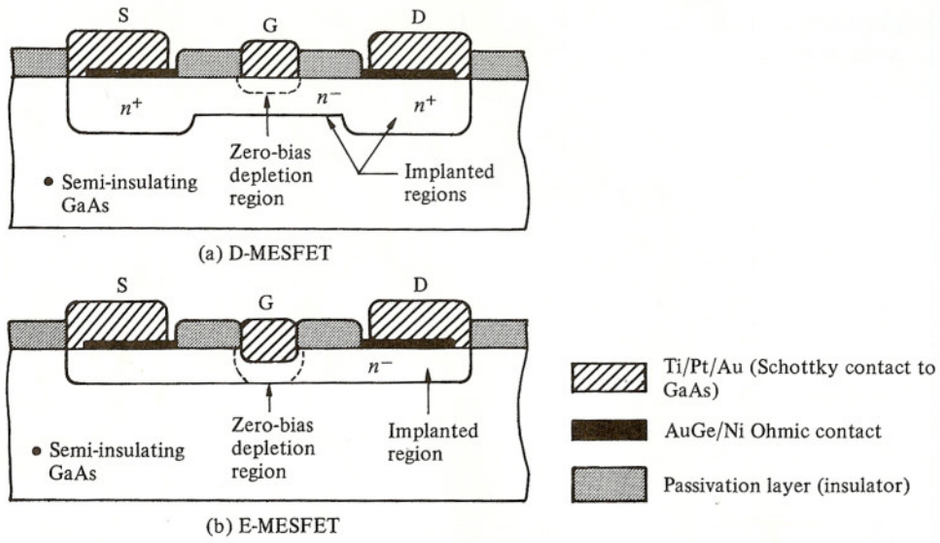

Figure 15.21 GaAs MESFET structure types. (a) Depletion-mode or D-MESFET; (b) enhancement-mode or E-MESFET.

in Fig. 15.21. Similar to the previously described J-FET, a bias applied to the gate of a D-MESFET further depletes the subgate region and reduces the channel conductance. The E-MESFET, on the other hand, is fabricated so that the built-in voltage associated with the metal-semiconductor contact is sufficient to totally deplete the channel. A forward bias must be applied to the E-MESFET gate to reduce the depletion width and obtain a channel current. The preponderance of applications including MMICs involve analog circuitry and make exclusive use of D-MESFETs. Digital logic circuits incorporate both D- and E-MESFETs.

It should be noted that high operational frequencies necessitate the fabrication of devices with extremely short channel lengths. The gate or active channel length in commercial devices is routinely $\lesssim 1$ μm. The discrete GaAs MESFETs listed in the 1993 Hewlett-Packard catalogue of communications components, for example, are quoted to have a nominal gate length of 0.25 μm.

15.3.2 Short-Channel Considerations

Given the structural similarities between the MESFET and J-FET, the I_D–V_D theory developed for the J-FET could be applied with only minor modifications to the MESFET provided all derivational assumptions are satisfied. Unfortunately, some of the derivational assumptions are at best questionable for the typical short-channel MESFET. For one, the $L \gg a$ assumption and the associated gradual channel approximation are clearly suspect. Second, the electric field in the FET channel is implicitly assumed to be sufficiently low so that the carrier drift velocity is given by $v_d = \mu_0 \mathscr{E}_y$, where $|\mu_0|$ is the usual low-field mobility. However, if a drain voltage of $V_D = 1$ V is applied across a channel length of $L = 1$ μm, the *average* magnitude of the electric field in the channel will be $|\overline{\mathscr{E}_y}| = V_D/L = 10^4$ V/cm. Since $|\mathscr{E}_y|$ increases as one progresses down the channel toward the drain, the magnitude of the electric field near the drain will be even larger than the cited average. Referring to Fig. 3.4 in Part I, we find the electron drift velocity in Si is significantly different from the extrapolated linear dependence at an electric field of 10^4 V/cm. Failure of the low-field assumption occurs at an even smaller $|\mathscr{E}_y|$-value in GaAs.

In the following discussion, we examine three modifications to the long channel theory that have been proposed in the device literature. Each of the approximate short channel models has its validity limits and utility under certain conditions.

Variable Mobility Model

The nonlinear variation of v_d with $\mathscr{E}_y$ as the carriers progress down the MESFET channel can be approximately taken into account using Eq. (3.3) from Part I. Specifically, assuming Eq. (3.3) with $\beta = 1$ adequately models the v_d versus $\mathscr{E}$ dependence, one can write

$$v_d = \frac{\mu_0 \mathscr{E}}{1 + \dfrac{\mu_0 \mathscr{E}}{v_{sat}}} \tag{15.20}$$

and

$$\mu(\mathscr{E}) \equiv \left|\frac{v_d}{\mathscr{E}}\right| = \frac{|\mu_0|}{1 + \dfrac{\mu_0 \mathscr{E}}{v_{sat}}} \tag{15.21}$$

where $\mu(\mathscr{E})$ is the field-dependent mobility and v_{sat} is the saturation drift velocity. If $\mu(\mathscr{E})$ with $\mu_0 = -\mu_n$ and $\mathscr{E} \to \mathscr{E}_y = -dV/dy$ is now substituted for μ_n in Eq. (15.1) of the long-channel J-FET derivation, and subsequent equations are appropriately modified, one ultimately obtains

$$I_D = \frac{I_D(\text{long-channel})}{1 + \dfrac{\mu_n V_D}{v_{sat} L}} \qquad \ldots 0 \le V_D \le V_{Dsat} \tag{15.22}$$

I_D(long-channel) is the I_D computed using Eq. (15.9). Above pinch-off, I_D(long-channel) $\to I_{Dsat}$(long-channel) and $V_D \to V_G - V_P$. In addition, $2a$ must be replaced by a in the long-channel current equations if the MESFET is a single-gate structure as pictured in Fig. 15.20.

Examining Eq. (15.22), we note that the drain current is always reduced relative to the long-channel case. This is to be expected since $\mu(\mathscr{E}) \le \mu_n$. Also, V_D/L in the denominator

of Eq. (15.22) is just $|\overline{\mathscr{E}_y}|$. It is therefore reasonable to identify $\mu_n V_D/L = \mu_n|\overline{\mathscr{E}_y}|$ as the corresponding "average" drift velocity, $\overline{v_d}$. Equation (15.22) obviously reduces to the long-channel result if $\overline{v_d} \ll v_{sat}$.

Overall, the variable mobility model provides an acceptable description of the nonlinear v_d versus $\mathscr{E}_y$ dependence in the FET channel and is adequate as a first-order correction to the long-channel theory when treating FETs of moderate channel length (typically $L \gtrsim 10\ \mu m$). However, the model does not account for the failure of the gradual channel approximation if $L \sim a$. As a consequence, additional considerations are necessary to properly describe the observed characteristics of short-channel MESFETs.

Saturated Velocity Model

Current saturation in long-channel devices is always caused by a pinching-off or constriction of the channel near the drain. An alternative mechanism can give rise to current saturation in short-channel devices where the gradual channel approximation is no longer valid.

Suppose $|\mathscr{E}_y|$ in a short n-channel device is sufficiently large so that $v_d \to v_{sat}$ at a point $y_1 < L$ in the FET channel. With $v_d = v_{sat}$, the current flowing at the point y_1 will be

$$I(y_1) = qv_{sat}N_D Z[a - W(y_1)] \tag{15.23}$$

The continuity of the channel current requires $I(y)$ to be the same at all points in the channel and, in particular, $I(y > y_1) = I(y_1)$. Since $v_d = v_{sat}$ at $y = y_1$, there can be no further increase in v_d at points $y > y_1$. It therefore follows from Eq. (15.23) that, to satisfy the $I(y > y_1) = I(y_1)$ requirement, $W(y)$ must be constant for all $y_1 \le y \le L$ as envisioned in Fig. 15.22. In total contrast to the assumption made in the gradual channel approximation, the described behavior can occur only if there is an appreciable $\mathscr{E}_y$ field in the subgate depletion region, with some of the field lines terminating on charges external to the gated region as illustrated in Fig. 15.22. Moreover, even though the channel is only partially constricted, the drain current through the device pictured in Fig. 15.22 will have saturated. The application of a larger drain bias will merely cause the y_1 point in the chan-

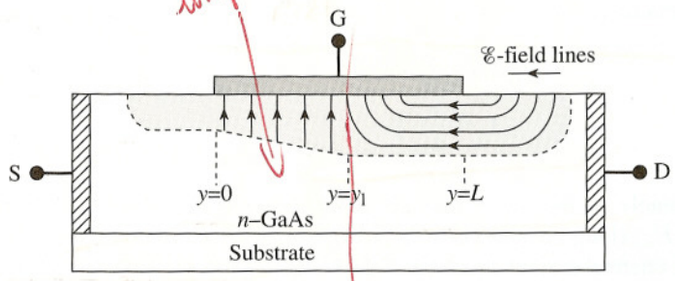

Figure 15.22 Approximate representation of the depletion region (shaded area) and electric field in a short channel MESFET where the drift velocity has reached its maximum value ($v_d = v_{sat}$) at the point y_1 in the channel.

nel to move closer to the source. In general, drain current saturation ($I_D = I_{Dsat}$) occurs when the channel pinches off *or* when $v_d \to v_{sat}$ at $y = L$.

If velocity saturation occurs in a MESFET with a channel length of only a few microns or less, then the depletion width in the $y_1 \le y \le L$ region of the device will differ by only a small amount from the depletion width at $y = 0$. For the envisioned special situation, $W(y_1)$ can be replaced by $W(0)$ in Eq. (15.23). This leads to the approximation

$$I_{Dsat} = I(y_1) \cong qv_{sat}N_D Z[a - W(0)] \tag{15.24}$$

with

$$W(0) = \left[\frac{2K_S\varepsilon_0}{qN_D}(V_{bi} - V_G)\right]^{1/2} = a\left(\frac{V_{bi} - V_G}{V_{bi} - V_P}\right)^{1/2} \tag{15.25}$$

Note that $W(0)$, the depletion width at $y = 0$, is computed assuming the gradual channel approximation can be applied to the source end of the channel. The saturation drain currents computed using Eqs. (15.24) and (15.25) are found to be in fairly good agreement with experimental results derived from short-channel ($L \sim 1\ \mu m$) GaAs MESFETs.

Two-Region Model

Although useful, the saturated velocity model provides only an expression for I_{Dsat}. The two-region model, on the other hand, provides an entire characteristic consistent with the saturated velocity model.

In the two-region model the analysis is broken into two parts corresponding to the two spatial or drift velocity regions pictured in Fig. 15.22. For $0 \le y \le y_1$ the gradual channel approximation and long-channel theory are assumed to hold *with* $v_d = \mu_0\mathscr{E}_y$ *throughout the region*. The $v_d = v_{sat}$ model is applied to the $y_1 \le y \le L$ portion of the channel. The transition point (y_1) is taken to occur at the y-value where $\mu_0\mathscr{E}_y = v_{sat}$. Naturally, the long-channel theory is applied throughout the channel if $\mu_0\mathscr{E}_{y|y=L} < v_{sat}$.

Paralleling the long-channel theory, the I_D–V_D characteristics are computed using Eq. (15.9) or the single-gate equivalent when $V_D \le V_{Dsat}$. Likewise, one sets $I_{D|V_D>V_{sat}} = I_{D|V_D=V_{sat}} \equiv I_{Dsat}$. However, in general $V_{Dsat} \ne V_G - V_P$ and Eq. (15.13) is *not* used to compute I_{Dsat}. In the two-region model, drain current saturation first occurs when $\mu_0\mathscr{E}_y = v_{sat}$ or $\mathscr{E}_y = v_{sat}/\mu_0$ at the drain end of the channel. If the long-channel relationships are solved for $V(y)$ in the channel (see Problem 15.3), the resulting expression differentiated with respect to y to obtain $\mathscr{E}_y$, and $V(L)$ equated to V_{Dsat} when $\mathscr{E}_{y|y=L} = v_{sat}/\mu_0 \equiv \mathscr{E}_{sat}$, one obtains

$$\mathscr{E}_{sat}L = \frac{V_{Dsat} - \frac{2}{3}(V_{bi} - V_P)\left[\left(\frac{V_{Dsat} + V_{bi} - V_G}{V_{bi} - V_P}\right)^{3/2} - \left(\frac{V_{bi} - V_G}{V_{bi} - V_P}\right)^{3/2}\right]}{\left(\frac{V_{Dsat} + V_{bi} - V_G}{V_{bi} - V_P}\right)^{1/2} - 1} \tag{15.26}$$

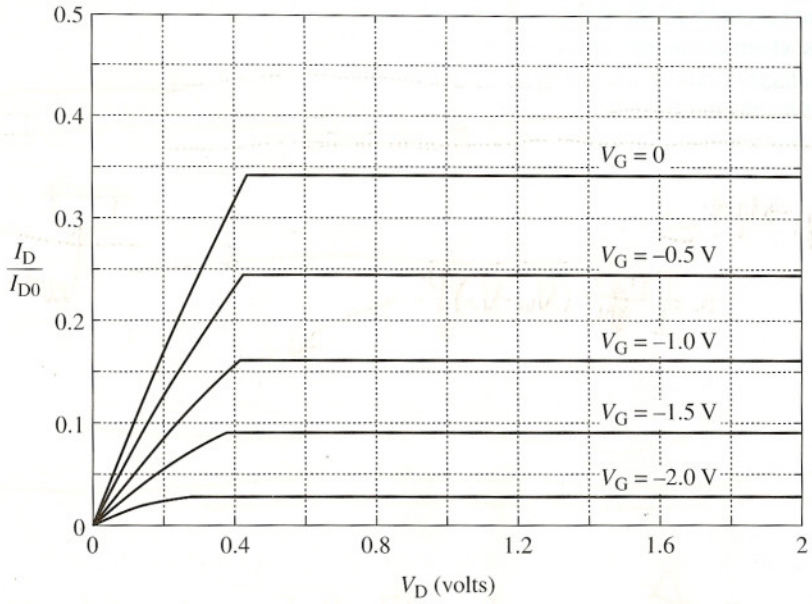

Figure 15.23 Normalized theoretical I_D–V_D characteristics of a short n-channel MESFET based on the two-region model. $V_{bi} = 1$ V, $V_P = -2.5$ V, $\mathscr{E}_{sat} = -5 \times 10^3$ V/cm, and $L = 1$ μm. The drain current is normalized to the $V_G = 0$ saturation current (I_{D0}) of an equivalent long-channel FET.

V_{Dsat} for a given V_G and set of device parameters is determined from a numerical solution of Eq. (15.26).

A sample set of theoretical I_D–V_D characteristics based on the two-region model is displayed in Fig. 15.23. An $\mathscr{E}_{sat} = -5 \times 10^3$ V/cm appropriate for GaAs n-channel MESFETs and $L = 1$ μm was assumed in establishing the characteristics. For comparison with long-channel results, the characteristics were normalized to $I_{D0} = I_{Dsat|V_G=0}$ computed using the single-gate version of Eq. (15.13).

Examining Fig. 15.23 we note that V_{Dsat} for most V_G values occurs at a significantly lower voltage and I_D/I_{D0} is reduced relative to the comparable long-channel characteristics presented in Fig. 15.16. Also, I_{Dsat} exhibits a V_G dependence approximately described by Eq. (15.24). Although somewhat crude in appearance with a noticeable discontinuity in slope at $V_D = V_{Dsat}$, the characteristics resulting from the two-region model afford a reasonable first-order match to the observed short-channel characteristics. It should be acknowledged, however, that an accurate modeling of the short-channel characteristics inherently requires the numerical two-dimensional solution of the electrostatic and current equations.